OPTIMIZED SPEED AND CURRENT CONTROLLER BASED HIGH SPEED SWITCHED RELUCTANCE MOTOR FOR EV APPLICATIONS

Abstract

The idea of recharging electric vehicles (EVs) using photovoltaic (PV) solar cells is novel and offers several technical and monetary benefits. This research offers a technological configuration of low-noise Switched Reluctance Motor (SRM) drives for EV applications. Due to growing ethical and affordable concerns about permanent magnet machines, there is a technical trend to employ SRMs in a number of mass production businesses. The PV panel supplies power to the SRM of the EV system. The Boost converter helps to improve the PV system's output, which is managed by Proportional Integral (PI) Controller. Using a Grey Wolf Optimization (GWO) based PI controller for SRM, the ideal parameter quantities for the EV system can be determined. The regulated DC voltage for the SRM has be provided by n+1 semiconductor and n+1 diode topology. The suggested method therefore shows the viability and efficacy of utilizing GWO as well as SRM optimization approaches for optimal tuning, resulting in better EV system performance. The recommended topology acts perfectly according to the findings of the suggested method's simulation in MATLAB.

Keywords: SRM, GWO, EV, PV System, PI Controller.

Authors

N. Kumarasabapathy
Assistant Professor
Department of Electrical and Electronics Engineering
Anna University Regional Campus
Tirunelveli, Tamil Nadu, India
nkumarautc@gmail.com

K. S. Kavin
Research Scholar
Department of Electrical and Electronics Engineering
Government College of Engineering
Tirunelveli, Tamilnadu, India
kavinksk@gmail.com

K. Sakthidhasan
Assistant Professor
Department of Electrical and Electronics Engineering
Vel Tech Multi Tech Dr. Rangarajan Dr. Sakunthala Engineering College
India
iesakthi@gmail.com

G. W. Martin
Associate Professor
Department of Electrical and Electronics Engineering
Marthandam College of Engineering and Technology
Tamil Nadu, India
gwmartinme@gmail.com

I. INTRODUCTION

Electric vehicles (EV) lay the foundation for environmentally friendly transportation. Undoubtedly, EV aids in the development of a low-carbon economy in the future.Due to the worsening air quality, EVs are proving to be less hazardous to the environment and energy efficient. As a result, the quantity and demand of EVs are growing daily, as well as the need for charging stations. The majority of charging stations are grid-connected, which adds to the grid's load and eventually highlights the need for charging stations powered by renewable energy[1].Charging EVs using PV panels would be a terrific choice and a long-term environmental move as sun has a vast potential for collecting power from PV panels[2]. Free energy from the sun has significant economic value and nearly no ongoing maintenance costs. Sunlight is safer and never runs out. Of course, solar energy is also more plentiful than fossil fuels[3].

The SR motor has a significant affinity to this field since it uses only high silicon steel and copper windings and does not use permanent magnets. Since there are several switches on the asymmetrical bridge converter used to control SR motors, power loss and negative torque current are enhanced[4].The control of a reluctance SRM developed for vehicle propulsion has been constructed with a high performance, completely digital controller. The controller is quilted to reduce torque ripple at low speeds, increase machine efficiency, and support peak overload conditions. Due to its exceptional performance and rare-earth-free nature, the SRM is becoming increasingly popular for EVs. Furthermore, it is demonstrated that the SRM may give a lengthy constant-horsepower operation with this flawless control, but the SRM's main flaw, particularly its enormous torque ripples, is solved [5].PV systems frequently use the switching power of DC-DC converters to create DC electricity and make place for SRM.

The many classes of single inductor DC-DC converters. The Boost converter has been determined to be the most suited candidate among all DC-DC converters due to its capacity to operate at its best regardless of the load side values[6].The (n+1) semiconductor and (n+1) diode send the Boost converter output to the SRM. The PI controller for the boost converter is designed primarily for operation during a start-up burst and continuous operation [7].

A PI Controller is a type of feedback controller that operates the plant by calculating the weighted total of the error and its integral. The fundamental purpose of a PI controller is to improve system performance in the face of interruptions, and the continuous operation of the PI controller has been improved by delivering feedback to the converter to cancel out the disturbances. However, the P-I controller has significant drawbacks, including unwanted speed overshoot, slow response caused by an abrupt change in load torque, and sensitivity to controller gains[8]. Therefore, algorithmic approaches are used to adjust the PI controller parameters. Particle Swarm Optimization (PSO), a population-based optimization algorithm method, suffers from the issue of premature convergence, which results in a poor convergence level, especially when handling challenging multi-peak search problems. This could make it less able to tackle challenging optimization issues[9]. In order to provide a reliable speed control for SRM, a new evolutionary method known as the GWO algorithm is suggested in this study. For the best possible design of the SRM's speed control, GWO is illustrated.

The main driver behind using GWO to remedy the shortcomings of SRM is the advancement of swarm computing approaches. The GWO algorithm is based on the natural behaviors of grey wolves. A unique augmentation for the GWO algorithm is developed and used to a PV system to improve its performance because GWO has fewer operators and parameters. The GWO Technique is used to change the PI controller's parameters to improve gain optimization[10].

The output of the PV system is enhanced using a Boost converter in this work under the direction of a PI controller, and a continuous power supply from a Boost converter is provided to SRM. The regulated voltage will be sent to the SRM using an n+1 semiconductor and n+1 diode arrangement. The GWO-PI controller is used to optimize the SRM speed control.

The structure of this work is as follows: In the second section, similar works are suggested. In the third section of the current work, the suggested system is explored in greater detail. The study's results are summarized in Section fourth.

II. RELATED WORKS

1. **Qingguo Sun *et al* (2023)** have created a solar-assisted SRM drive with great integration for EV applications. Standard switch modules are employed, providing substantial advantages for optimum heat transfer layout and mass production of SRM drives for EVs. The Boost converter, which has high power factor adjustment capabilities, may charge the battery pack as well as serve as a discharge source for loads that are flexible coordinated with the PV panels. However, the structure's intricacy and production costs rise. Although existing approaches may greatly reduce circumferential noise and torque ripple, other performance characteristics such as torque and efficiency suffer.

2. **Mahmoud A. Gaafar *et al* (2022)** have suggested a method for determining the appropriateness of the converters for use in SRM-based EV systems. As a result, the converters are graded differently to reflect their cost differences as well as their technical influence on the SRM system. For EV applications, the results offer a good indicator of the trade-off between getting certain benefits and sacrificing others. Although present methods reduce circumferential noise significantly, other performance metrics such as speed and effectiveness suffer.

3. **Vinícius Augusto De Abreu Batista *et al* (2023)** suggested a method to assure optimal SRM performance. Following the conclusion of the optimization process, sensitivity studies are done to evaluate the impact of driving angles on the performance of the SRM. The findings demonstrate that the suggested enhancement approach is successful in establishing the suitable control settings across a wide range of operation speeds. However, it will not be able to regulate the speed of SRM.

4. **Yuanfeng Lan*et al* (2022)** have suggested a boost converter for SRM, as well as an analytical calculation approach for it. Each traditional asymmetric half-bridge driver in the proposed converter features a passive front-end circuit. T maximize torque, optimization methods are employed to regulate the planned SRM drive. Furthermore, they suggest optimization opportunities based on the cost and technical performance of

various SRM converters. Noise and vibration reductions across a large speed range have not been efficiently attained in existing control systems.

5. **Alisha Ahmed *et al* (2018)** have suggested the use of Grey Wolf Optimization (GWO) for efficient speed management of a DC motor. For selecting the settings of the PID controller, GWO employed the integral of time multiplied absolute error (ITAE) as an objective function. The proposed GWO/PID strategy was also compared to other existing approaches. With modifications in DC motor parameters, the robustness and comparative analysis of the proposed GWO/PID approach were also done.Variations in the characteristics of the DC motor have been shown to have no effect on the functioning of the PID controller.

III. PROPOSED SYSTEM

The system comprises of a PI-controlled Boost converter, n+1 semiconductors and n+1 diodes, and a GWO-PI controller to adjust the speed of the SRM. The GWO optimization is used to find the most effective configuration in order to provide reliable speed control for SRM. The GWO method is used to assess the PI controller settings, and the output response is delivered to the SRM. The proposed technique for enhancing the SRM using GWO-PI Controller is shown in the Figure 1.

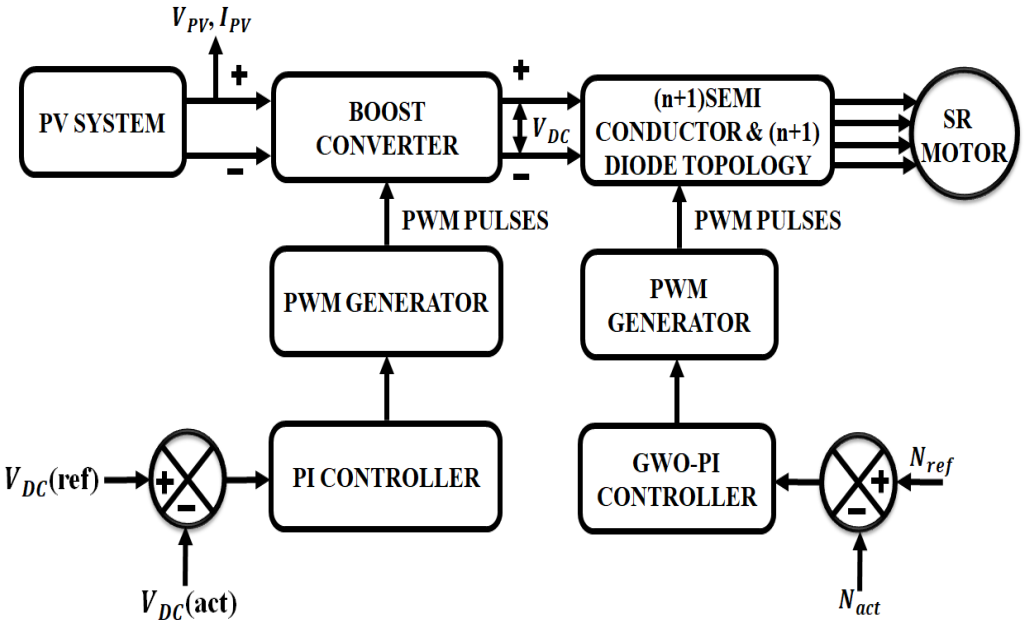

Figure 1: SRM using GWO-PI Controller

Under the management of a PI controller, a Boost converter is used to increase the PV system's output, and a PI based Boost converter is used to feed SRM with continuous power. When the operating point fluctuates, Boost converters are utilized to augment the dynamics of current management under the supervision of PI.An n+1 semiconductor and n+1 diode configuration is used to deliver the regulated voltage to the SRM. To maximize the SRM speed control, the GWO-PI controller is employed.

1. **PV System:** Electricity is produced directly from sunlight via PV panels. The photon traveling in the electromagnetic wave is how the sun's energy reaches the planet. The electrons (negative charge), which are energized and leave the holes (positive charge), in semiconductor material as the light strikes the solar cell. More electron mobility is produced when the absorbed light has a greater energy level. The traveling electrons carry the charge, and electricity is produced. When electron movements get longer, more electricity is created. Recombination, which occurs when an electron returns to its hole, makes it desirable for the material used in solar cells to keep electron-hole pairs alive for as long as possible. When an electron recombines, its whole companion is destroyed, and no power is produced. Each of the components depicted in Figure 2's systematic diagram of a PV system contributes to the decrease in efficiency.

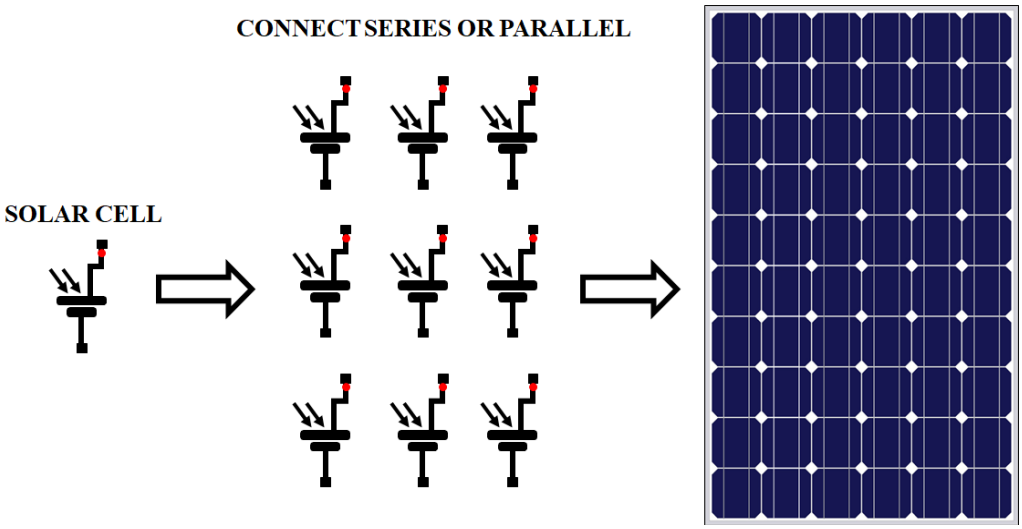

Figure 2: Topology of PV System

When solar radiation reaches the surface of PV panels, it generates direct current (DC), classifying solar cells as a semiconductor device. A diode and two resistances are present. Figure 3 depicts the topology of the PV system's structure. The R_S depicts the losses, which are connected with p-n junction, semiconductor components. The R_P parallel reflects the loss produced by a small leakage current flowing via the parallel channel. The current of the solar panel array is denoted byI_L. The reverse saturation current of a PV array is denoted by I_O, while the electron charge is denoted by q.

$$I_{Out} = I_{sc} - I_D \tag{1}$$

$$I_D = I_O * \left(e^{q.\frac{v+lR_S}{nKT}} + 1\right) \tag{2}$$

$$I_{Out} = I_L - I_O * (e^{q.\frac{v+lR_S}{nKT}} + 1) - \frac{V+R_S*1}{R_P} \tag{3}$$

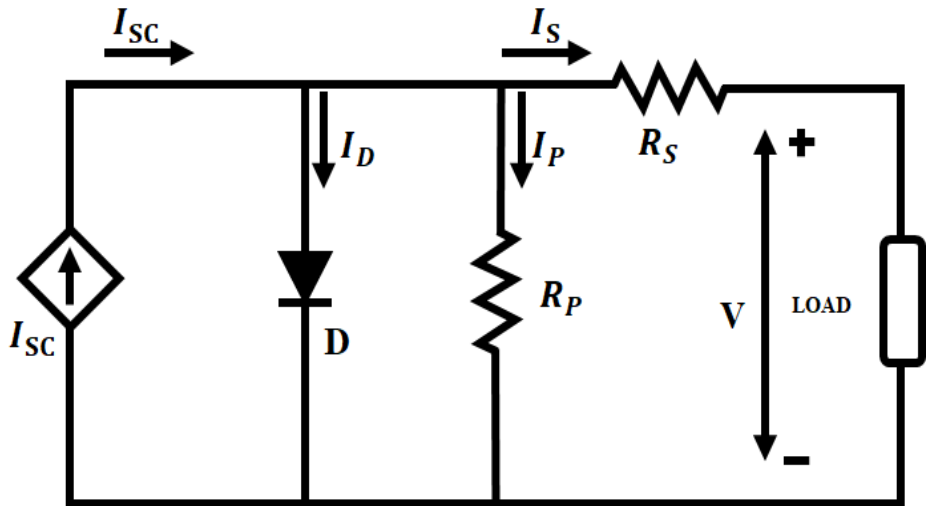

Figure 3: PV circuit

2. **Boost Converter:** A boost converter is used to increase the voltage from the source to the target value. This converter may accept input from any DC source, such as a solar panel or batteries. Figure 1 depicts the boost converter circuit schematic.

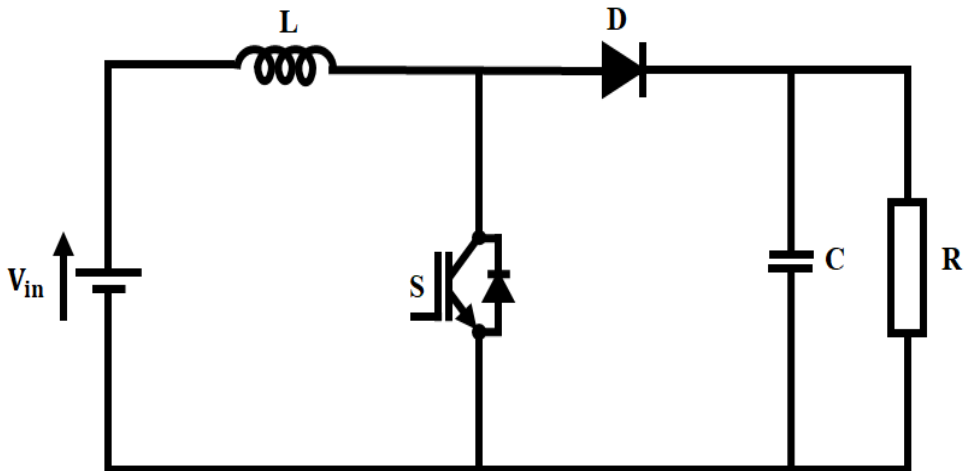

Figure 4: Boost Converter Circuit

In continuous mode, the boost converter has two alternative architectures, as shown in Figure.

- Switch S is switched off in the off-state. The stored energy in the inductor reverses polarity to charge the capacitor via the diode.
- Switch S is in the on position. The supply voltage charges the inductor, which stores the energy. The inductor current progressively increases during this stage.

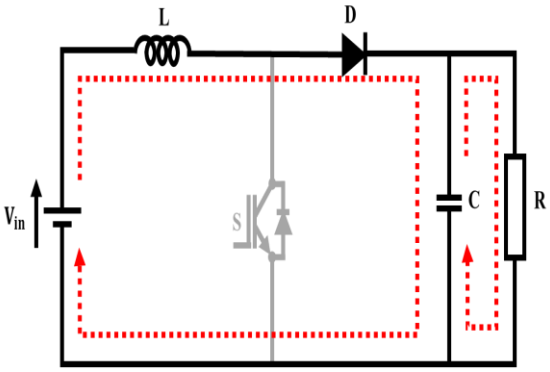

Figure 5a: Mode 1

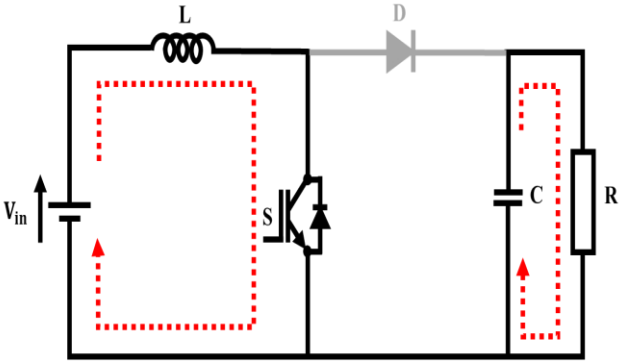

Figure 5b: Mode 2

Initially, the voltage is kept constant, and then it is sent back to the boost regulator through the PI controller and PWM generator. A boost converter is used to convert a direct current source to a direct current source. Essentially, the solar panel converts heat energy into direct current voltage. The PI controller maintains a steady output voltage; it is used to control the output voltage. The PWM generator is utilized to commutate the MOSFET angle. The error signal is received from the comparator. Again, the output voltage is obtained constantly as a constant output voltage.

The mathematical formula for inductance voltage equalization

$$V_g(DT_S) + (V_S - V_O)(1-D)T_S = 0 \quad (4)$$

$$V_O = V_g/(1-D) \quad (5)$$

Conversion Ratio, $M = V_O/V_g = 1/(1-D)$ (6)

Change in inductor current based on inductor current ripple analysis

$$\Delta I_i = (I_{max} - I_{min}) \quad (7)$$

$$\Delta I_L = (V_g/L) * (DT_S) \quad (8)$$

$$L = (V_g D/f_S(\Delta I_L) \quad (9)$$

Here Boost converters is employed under the supervision of PI to increase the dynamics of current management since the tiny signal model changes when the operating point fluctuates. The PI controller is designed to work with the boost converter during its initial transient and constant state.

3. **SRM:** A machine with a synchronous output is a reluctance motor. Its stator windings are coiled field coils from a DC motor, and it has no coils or magnets on its rotor. The stator and rotor both contain prominent poles, indicating that the machine is doubly salient. When the diametrically opposing stator poles are energized, the rotor is aligned.

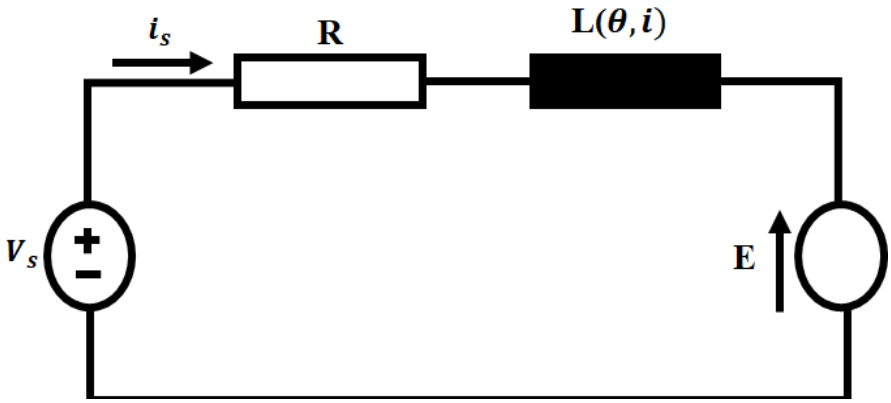

Figure 6: SRM Equivalent Circuit

Because of the saturation property of magnetic material, the value of inductance differs not merely changing rotational angle θ but additionally with current across winding. As a result, the usual form of the inductance equation is $L = L(\theta, i)$, where $\theta$the angle of rotation of the rotors isand i is the phase current. As a result, the typical formulation for total linkage fluxes in the motor is as follows.

$$\lambda(\theta, i) = L(\theta, i).i \tag{10}$$

Figure 3 depicts the comparable circuit for one phase of the SRM. The total flux expression is as follows.

$$\lambda(\theta) = L(\theta).I \tag{11}$$

A phase current in SRM enabling continuous processing. The co-energy corresponds to the magnetic field energies accumulated in the linear region.

$$W_m = W_m^{'} = \int_0^i \lambda(i, \theta).di = L(\theta).i^2/2 \tag{12}$$

$$W_m = \frac{1}{2}\int H.B.dv \tag{13}$$

The torque generated by rotor position is expressed as,

$$T=[\partial W_m^{'}/\partial\theta]i = \text{Const} \tag{14}$$

However, the current regulator is an essential component of the control block. To accomplish this, a totally digital PI current regulator is employed to control the phase current of the SRM. Due to the SRM's exceedingly nonlinear and non-sinusoidal operation, a straightforward implementation of a PI regulator is almost difficult. To overcome this, an improved PI controller is used.

4. **GWO-PI Controller:** The suggested GWO algorithm optimizes the PI controller to provide the optimal control performance, that is, low overshoot and quick rise and

adjustment times. The GWO algorithm is capable of improving system control quality and achieving the intended result.

GWO is a nature-inspired process that utilizes wolf hunting activity. Searching for, surrounding, and assaulting prey. Grey wolves often live in packs of five to twelve animals. As indicated in Figure, the groupings are generally divided into four members α,β,δ, and ω wolf. Wolves ω prey on the young members of the pack.

$$\vec{D}_{GWO} = \left|\vec{C}_{GWO}.\ \ \vec{X}_P(it) - \vec{X}\ (it)\right| \tag{15}$$

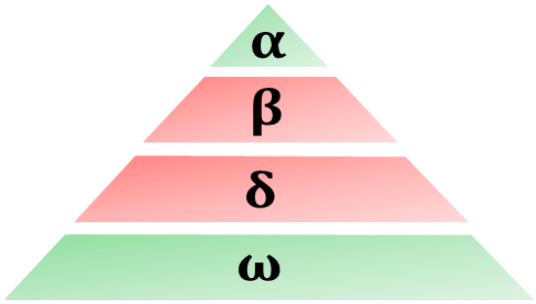

Figure 7: GWO

The grey wolves' first three ideal positions are

$$\vec{X}_1 = \vec{X}_\alpha\ - \vec{A}_1.\ (\vec{D}_\alpha) \tag{16}$$

$$\vec{X}_2 = \vec{X}_\beta\ - \vec{A}_2\ .(\vec{D}_\beta) \tag{17}$$

$$\vec{X}_3 = \vec{X}_\delta\ - \vec{A}_3.\ (\vec{D}_\delta) \tag{18}$$

The following is the formula for updating the prey positions:

$$\vec{X}\ (it+1) = \frac{\vec{X}_1 + \vec{X}_2 + \vec{X}_3}{3} \tag{19}$$

The GWO optimization is employed for the best feasible design in order to give a dependable speed control for SRM. The PI controller settings are evaluated using the GWO algorithm, and the output response is sent to the SRM.

5. **n+1 Semiconductor and n+1 Diode Topology:** The interleaved boost converter signal is sent to the SRM through the (n+1) semiconductor and (n+1) diode. This architecture minimizes converter costs by using fewer switching components, which reduces losses across a wider range. All switching devices and diodes have a lower rating.

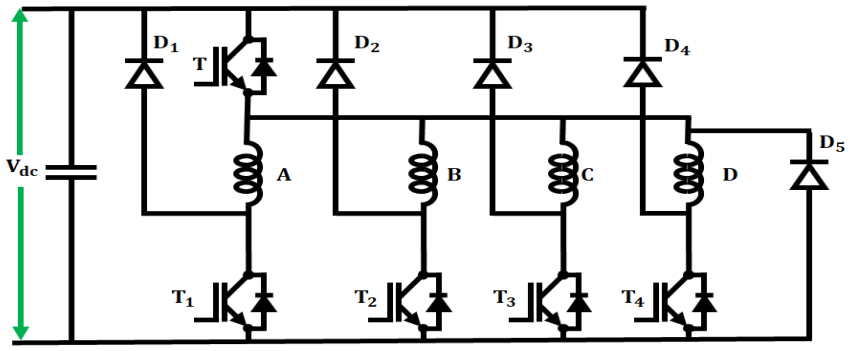

Figure 8: Circuit Layout of n+1 Semiconductor and n+1 Diode

When the switches are closed, the phase winding A is powered by the input DC supply. When the switches are opened, the energy from phase winding A is returned to the mains through diodes. When the switches are opened, the stored energy in B is returned to the mains. When the switches are closed, C is also engaged. When these switches are opened, the energy held in C is restored to the mains. When the switches are closed, the phase winding D is powered up. When the switches are opened, the stored energy in D is restored to the mains. This circuit employs (n+1) diodes and (n+1) power switching devices, with n denoting the number of phases.

IV. RESULTS AND DISCUSSION

1. **PV Waveform:** In this stage, the installation is stimulated using MATLAB to test the SRM. Figures depict the characteristic curves of the PV panels in relation to temperature and insolation parameters in the proposed PV system.

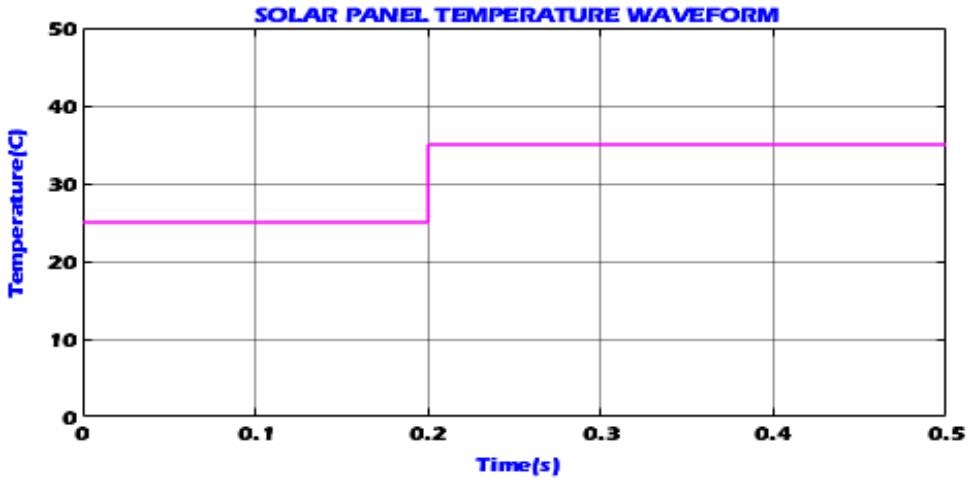

Figure 9:PV Temperature Waveform

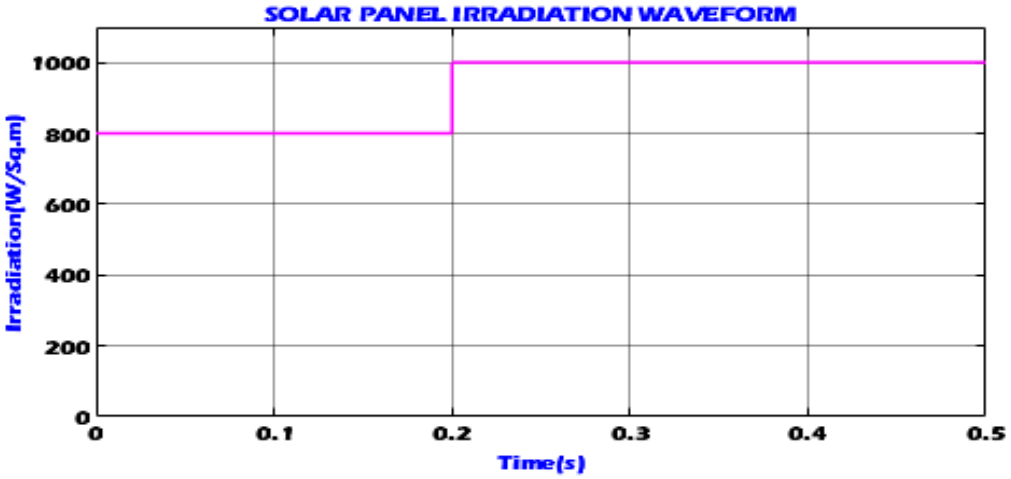

Figure 10: PV Irradiation Waveform

Figures 9 and 10 display the temperature waveform and irradiance waveform of a solar panel, respectively. The temperature and irradiance in this waveform are both constant at 25°C and 800(W/sq-m), respectively.

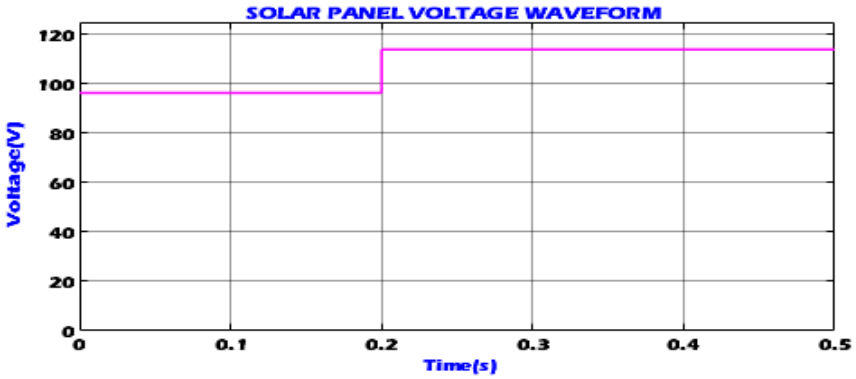

Figure 11: PV Voltage Waveform

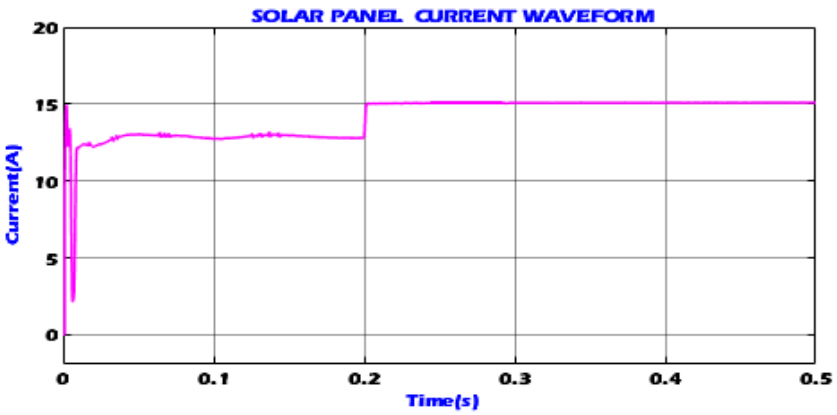

Figure 12: PV Current Waveform

Figures 11 and 12 depict the voltage waveform and current waveform of a solar panel, both of which show that the voltage stays constant at 118 V and the current stays constant at 15 A after the settling time of 0.2s.

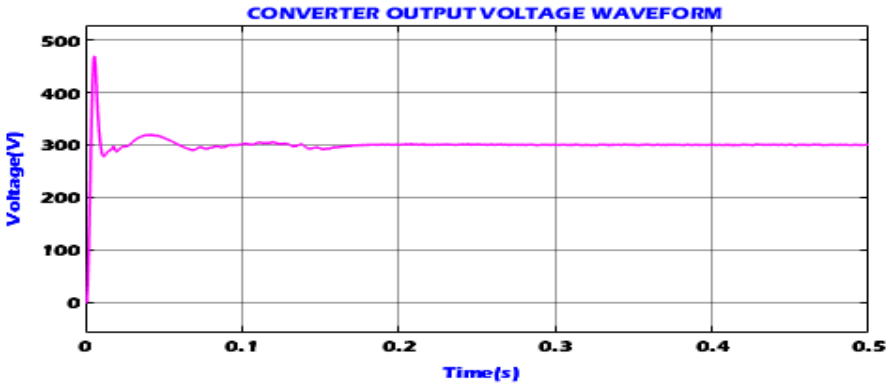

Figure 13: Output Voltage of Converter

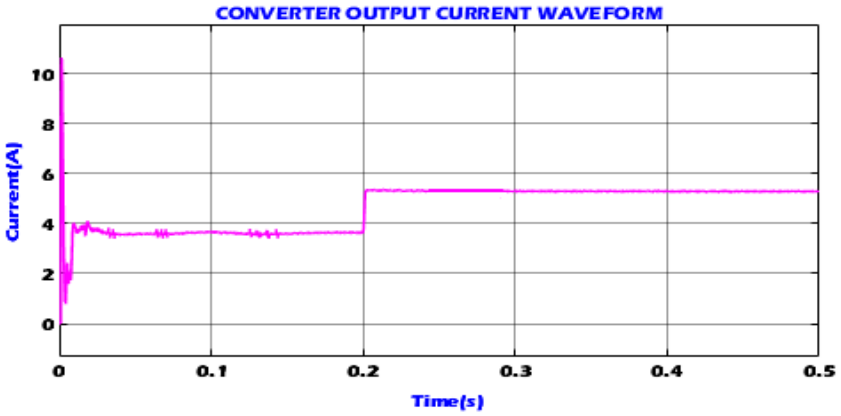

Figure 14: Output Current of Converter

The converter output voltage Waveform and current output waveform in Figure 13 and 14 shows that the current remains constant after 0.2 s with a value of 5.8 A and the voltage slightly varies up to 0.2s after that it remains constant at the value of 300 V.

2. **SRM Waveform:** The suggested SRM is modelled in Matlab.GWO-PI controllers are designed and modelled to manage the speed of the srm as well as the input voltage. In srm, the simulated results demonstrate controlled output voltage and steady speed.

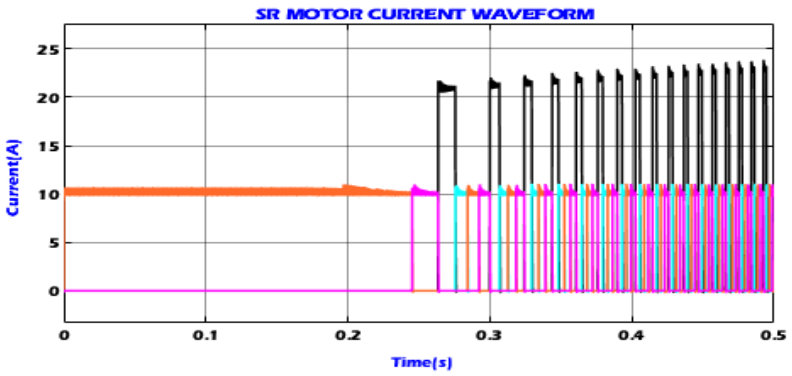

Figure 15:SR Motor Current Waveform

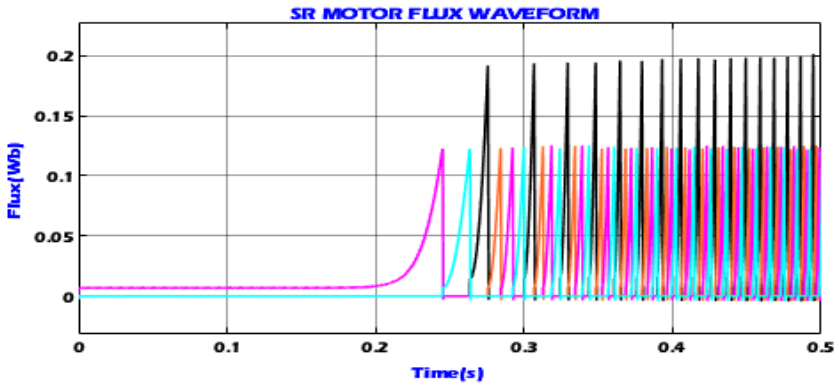

Figure 16:SR Motor Flux Waveform

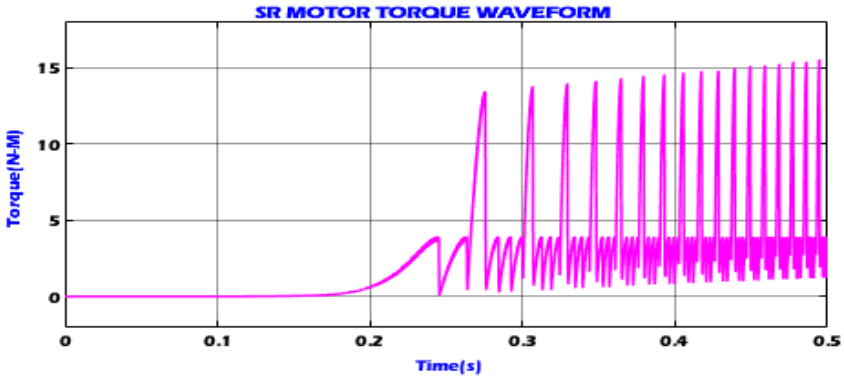

Figure 17: SR Motor Torque Waveform

Figures 15, 16, and 17 show the SRM waveforms of current, flux, and torque, which indicate that it remains constant upto 0.2s before varying.

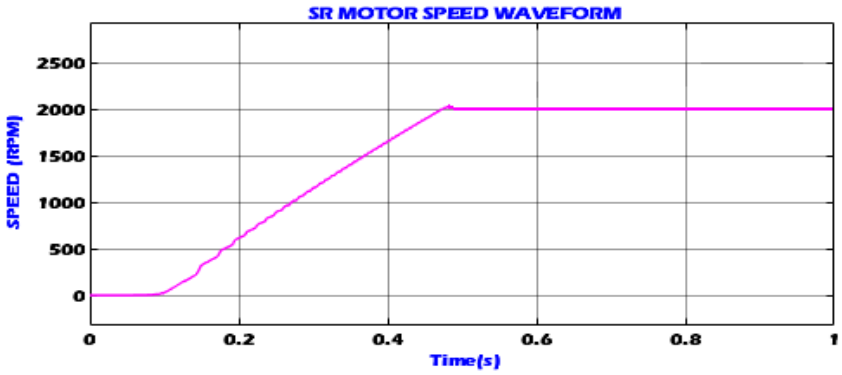

Figure 18:SR Motor Speed Waveform

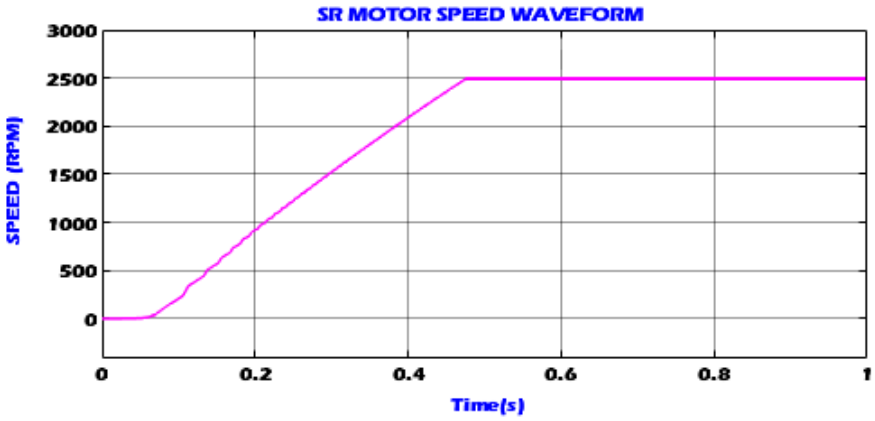

Figure 19: SR Motor Speed Waveform

Figures 18 and 19 indicate that the SRM maintains a steady speed of 2000rpm and 2500rpm under varying loads.

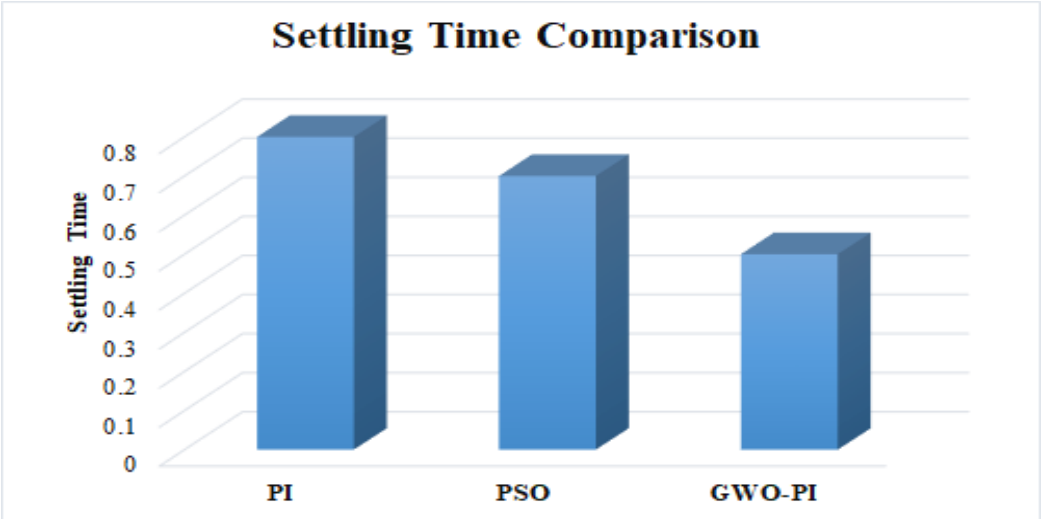

Figure 20: Setting Time Comparison

Figure 20 exhibits a settling time comparison of PI,PSO-PI, and GWO-PI, demonstrating that our proposed GWO-PI achieves constant speed with minimal settling time.

V. CONCLUSION

Optimizing the SRM system to decrease noise and vibration is critical for EV applications. A GWO-PI Controller for SRM is built and emulated in order to regulate SRM input voltage and manage SRM speed. The output analysis indicates that the Boost converter can boost the voltage even with a low input voltage to the other topology.At steady condition, the output voltage is enhanced and constant. The simulated output voltage and current waveform demonstrates the GWO-PI Controller's excellent responsibility. The SRM Speed waveform showed that SRM maintains a constant speed of 2000rpm and 2500rpm under various loads with a settling time of 0.5s.

REFERENCES

[1] Hannan, Mahammad A., Md Murshadul Hoque, Aini Hussain, Yushaizad Yusof, and Pin Jern Ker. "State-of-the-art and energy management system of lithium-ion batteries in electric vehicle applications: Issues and recommendations." *Ieee Access* 6 (2018): 19362-19378.

[2] González-Castaño, Catalina, Carlos Restrepo, Samir Kouro, and Jose Rodriguez. "MPPT algorithm based on artificial bee colony for PV system." *IEEE Access* 9 (2021): 43121-43133.

[3] Nwaigwe, K. N., Philemon Mutabilwa, and Edward Dintwa. "An overview of solar power (PV systems) integration into electricity grids." *Materials Science for Energy Technologies* 2, no. 3 (2019): 629-633.

[4] Ahn, Jin-Woo, and Grace Firsta Lukman. "Switched reluctance motor: Research trends and overview." *CES Transactions on Electrical Machines and Systems* 2, no. 4 (2018): 339-347.

[5] Xu, Aide, Chaoyi Shang, Jiagui Chen, Jingwei Zhu, and Lele Han. "A new control method based on DTC and MPC to reduce torque ripple in SRM." *IEEE Access* 7 (2019): 68584-68593.

[6] Sadaf, Shima, Mahajan Sagar Bhaskar, Mohammad Meraj, Atif Iqbal, and Nasser Al-Emadi. "A novel modified switched inductor boost converter with reduced switch voltage stress." *IEEE Transactions on Industrial Electronics* 68, no. 2 (2020): 1275-1289.

[7] Gheisarnejad, Meysam, and Mohammad Hassan Khooban. "Design an optimal fuzzy fractional proportional integral derivative controller with derivative filter for load frequency control in power systems." *Transactions of the Institute of Measurement and Control* 41, no. 9 (2019): 2563-2581.

[8] J. Zhang, L. Li, D. G. Dorrell and Y. Guo, "Modified PI controller with improved steady-state performance and comparison with PR controller on direct matrix converters," in Chinese Journal of Electrical Engineering, vol. 5, no. 1, pp. 53-66, March 2019.

[9] Shami, Tareq M., Ayman A. El-Saleh, Mohammed Alswaitti, Qasem Al-Tashi, Mhd Amen Summakieh, and Seyedali Mirjalili. "Particle swarm optimization: A comprehensive survey." *IEEE Access* 10 (2022): 10031-10061.

[10] A. K. Mishra, S. R. Das, P. K. Ray, R. K. Mallick, A. Mohanty and D. K. Mishra, "PSO-GWO Optimized Fractional Order PID Based Hybrid Shunt Active Power Filter for Power Quality Improvements," in IEEE Access, vol. 8, pp. 74497-74512, 2020, doi: 10.1109/ACCESS.2020.2988611.

[11] Q. Sun, H. Xie, X. Liu, F. Niu and C. Gan, "Multiport PV-Assisted Electric-Drive-Reconstructed Bidirectional Charger With G2V and V2G/V2L Functions for SRM Drive-Based EV Application," in IEEE Journal of Emerging and Selected Topics in Power Electronics, vol. 11, no. 3, pp. 3398-3408, June 2023, doi: 10.1109/JESTPE.2023.3240434.

[12] M. A. Gaafar, A. Abdelmaksoud, M. Orabi, H. Chen and M. Dardeer, "Switched Reluctance Motor Converters for Electric Vehicles Applications: Comparative Review," in IEEE Transactions on Transportation Electrification, 2022, doi: 10.1109/TTE.2022.3192429.

[13] V. A. De Abreu Batista, M. V. De Paula, P. R. Melo Costa, B. A. De Oliveira and T. A. Dos Santos Barros, "Multiobjective Grey Wolf Optimization of Firing Angles for SRM Drives," 2023 IEEE Transportation Electrification Conference & Expo (ITEC), Detroit, MI, USA, 2023, pp. 1-6, doi: 10.1109/ITEC55900.2023.10186975.

[14] Y. Lan, J. Croonen, K. Deepak, Y. Benomar, M. E. Baghdadi and O. Hegazy, "Turn-off Angle Analytical Calculation Method of a Passive Boost Converter with Parallel Type Capacitors for Switched Reluctance Motors," 2022 IEEE 20th International Power Electronics and Motion Control Conference (PEMC), Brasov, Romania, 2022, pp. 321-326, doi: 10.1109/PEMC51159.2022.9962900.

[15] H. Shayeghi, R. Mohajery, N. Bizon, P. Thounthong and N. Takorabet, "Implementation of PD-PI Controller for Boost Converter Using GWO Algorithm," 2022 14th International Conference on Electronics, Computers and Artificial Intelligence (ECAI), Ploiesti, Romania, 2022, pp. 1-7.

